

# Implicit Pairs for Boosting Unpaired Image-to-Image Translation

Yiftach Ginger  
Tel Aviv University  
iftachg@mail.tau.ac.il

Dov Danon  
Tel Aviv University  
dov84d@gmail.com

Hadar Averbuch-Elor  
Tel Aviv University  
hadar.a.elor@gmail.com

Daniel Cohen-Or  
Tel Aviv University  
dcor@tau.ac.il

## Abstract

*In image-to-image translation the goal is to learn a mapping from one image domain to another. In the case of supervised approaches the mapping is learned from paired samples. However, collecting large sets of image pairs is often either prohibitively expensive or not possible. As a result, in recent years more attention has been given to techniques that learn the mapping from unpaired sets.*

*In our work, we show that injecting implicit pairs into unpaired sets strengthens the mapping between the two domains, improves the compatibility of their distributions, and leads to performance boosting of unsupervised techniques by over 14% across several measurements.*

*The competence of the implicit pairs is further pronounced with the use of pseudo-pairs, i.e., paired samples which only approximate a real pair. We demonstrate the effect of the approximated implicit samples on image-to-image translation problems, where such pseudo-pairs may be synthesized in one direction, but not in the other. We further show that pseudo-pairs are significantly more effective as implicit pairs in an unpaired setting, than directly using them explicitly in a paired setting.*

## 1. Introduction

The goal of image-to-image translation is to learn a mapping from one image domain to another. In recent years, a plethora of methods has arisen to solve the problem using deep neural networks. A straightforward supervised approach is to learn the mapping from paired samples [11]. However, collecting large sets of image pairs is often prohibitively expensive or infeasible. Learning the mapping from unpaired data is thus more attractive, but significantly more technically challenging, as the problem becomes highly under-constrained. A common solution is to limit the space of possible mappings to those that obey circularity constraints [29, 28, 14].

Bridging the gap between paired and unpaired training,

Tripathy et al. [21] propose a hybrid framework that simultaneously considers paired and unpaired image samples. In their work, they demonstrate that training explicitly on the paired samples and implicitly on unpaired ones yields a boost in performance compared to unsupervised, unpaired, techniques. In our work, we define *implicit pair* as a pair that exists in the training data, but is not used explicitly in the training process. We argue that training in an unsupervised manner on such *implicitly* paired data would improve the performance compared to training on unpaired data.

Through extensive experiments we analyze in this paper the power of implicit pairs in an unpaired setting. Furthermore, we demonstrate that for this purpose, the implicit pairs can be pseudo-pairs, i.e., a pair in which one of the samples is synthetic as an approximation of a real pair and that even implicit *pseudo*-pairs still boost the performance of learning in an unpaired setting.

In this paper, we examine the strength of the implicit pseudo-pairs in an asymmetric setting. In this setting there is a process, or model, which allows estimation of the mapping from one domain to the other, but not in the opposite direction. Consider, for example, the domains *wearing eyeglasses* and *not wearing eyeglasses* which capture facial images where the subjects are distinguished by whether or not they are wearing eyeglasses. While a mapping from *not wearing eyeglasses* to *wearing eyeglasses* may be easy to approximate using a simple model-based synthesis technique, the inverse mapping does not have a simple model-driven solution.

We start the analysis by showing that the quality of the mappings learned depends on the portion of implicit pairs in the dataset. This non-intuitive finding encourages the exploration of using pseudo-pairs as implicit pairs in an unpaired setting. We demonstrate the effect of the approximated samples on image-to-image translation problems. We further argue that pseudo-pairs are significantly more effective when used as implicit pairs in an unpaired setting, than using them explicitly in a paired setting. Explicitly stated, our contributions are:

- We demonstrate that image-to-image translation networks benefit from the latent signal that implicit pairs add to the dataset.
- We analyze the effect of the percentage of pairs in the dataset and demonstrate that having even a small percentage of pairs enhances the datasets and allows the model to reach peak performance rates.
- We introduce pseudo-pairs to the image-to-image translation framework and demonstrate that pseudo-pairs are more effective in an unpaired setting than as explicit pairs in a paired setting.

## 2. Related Works

Pix2Pix [11] was the first successful attempt to use a conditional GAN to learn a mapping between two image distributions. As a supervised method it requires paired samples, one from each distribution, to be explicitly linked in the training phase.

As gathering a large paired dataset can be difficult and expensive, unsupervised architectures were suggested which do not require such explicit pairing [29, 17, 28, 14, 6].

Bridging the difference between supervised and unsupervised architectures, several methods allow the use of a small set of paired images, together with a large set of unpaired ones in a semi-supervised fashion. They accomplish this by alternating between supervised and unsupervised phases during training [12, 21]. Other semi-supervised solutions separate the learning of the joint distribution and the marginal distribution of the domains, by independently learning the from the supervised set and the unsupervised set [9, 16].

Deep neural networks require large amounts of data to train properly, which can prove prohibitively expensive in some cases. To cope with this problem various methods have been devised to create more samples by augmenting existing data into new samples in order to create meaningful expressions of the underlying distribution. Simple augmentation methods for images include rotation, skewing, cropping and other affine transformations. These simple methods are quite ubiquitous, but limited in the amount of data they can generate, as well as the amount of effective information that they add to the dataset.

Other more complex augmentation methods could be model-based, use learned generative models, and even GANs [24, 5, 22, 3, 26, 8, 19, 20].

Lastly, we are not aware of any prior work that use more advanced methods to augment a dataset that is used to train a GAN. This leaves this field restricted in ways that other ML domains are not.

## 3. Background and Outline

### 3.1. Paired and unpaired settings

Modern image-to-image translation models use GANs to obtain plausible images in the target domain. When using only an adversarial loss the translation problem is highly under-constrained. Thus, it could easily lead to mode collapse where the generator learns to fool the discriminator by producing images only from a small part of the target distribution.

To constrain the problem, the model can be trained using pairs, which are explicitly provided and used during training. In general, explicit-pairs constraints alleviate most of the problems of mode collapse. Learning with explicit pairs constitutes the paired setting.

A notable example for an algorithm that uses explicit pairs is the Pix2Pix algorithm [11] which learns a one-directional mapping by conditioning the discriminator and the generator on the given source and target pairs. More formally, to learn a mapping  $A \rightarrow B$ , the algorithm samples pairs  $(a, b) \in (A, B)$  and trains the generator and discriminator with the following adversarial loss function:

$$L_{cGAN}(G_{AB}, D_B) = \mathbb{E}_{a,b}[\log D_B(a, b)] + \mathbb{E}_a[\log(1 - D_B(a, G_{AB}(a)))] \quad (1)$$

where  $G_{AB}, D_B$  are the generator and discriminator, respectively. Pix2Pix uses the pairs to further constrain the mapping with an  $L1$  distance loss which requires the generated samples to be close to the ground-truth paired sample:

$$L_{L1}(G_{AB}) = \mathbb{E}_{a,b}[||b - G_{AB}(a)||_1]. \quad (2)$$

The full loss function is the combination of these functions:

$$L_{cGAN}(G_{AB}, D_B) + L_{L1}(G_{AB}) \quad (3)$$

There are many cases where it is difficult or even impossible to have paired samples. In such cases, the translation can be learned in an unpaired setting. In the unpaired setting there are two training sets, one for each domain, but the instances in the two domains are not explicitly related. They may contain pairs but in such a case their correspondence is not given, and therefore is not used in the loss function.

Various solutions have been proposed to better constrain the mapping in the severely under-constrained unpaired setting.

For example, in CycleGAN and DualGan [29, 28] the adversarial loss is combined with a cycle consistency loss. More formally, in CycleGAN the loss function is:

$$L_{GAN}^{A \rightarrow B} + L_{GAN}^{B \rightarrow A} + \lambda L_{cycle} \quad (4)$$

where the adversarial objective used to encourage plausible generated images in the target domain is:

$$L_{GAN}^{A \rightarrow B}(G_{AB}, D_B, A, B) = \mathbb{E}_{b \sim p_{data}(b)}[\log D_B(b)] + \mathbb{E}_{a \sim p_{data}(a)}[\log(1 - D_B(G_{AB}(a)))] \quad (5)$$

and the cycle consistency loss is defined according to:

$$L_{cycle}(G_{AB}, G_{BA}) = \mathbb{E}_{a \sim p_{data}(a)} [\|G_{BA}(G_{AB}(a)) - a\|_1] + \mathbb{E}_{b \sim p_{data}(b)} [\|G_{AB}(G_{BA}(b)) - b\|_1] \quad (6)$$

It should be stressed that the above algorithm does *not* use pairing information even if the training set consists entirely or partially of pairs.

### 3.2. Implicit pairs

The unpaired framework does not explicitly use any mutual information of paired data, which may exist in the unpaired sets. We argue that having paired data boosts the performance of the translation model even in the unpaired setting as the pairs describe the desired transformation, implicitly guiding the learning. In our experiments, we use partially paired datasets such that an  $\alpha$  portion of them are paired. For example, with  $\alpha = 0.25$ , a quarter of the samples are paired and the rest are unpaired.

In the paired setting it is assumed that  $\alpha = 1$  and  $|A| = |B|$ . While prior work ignored the possible existence of pairs, we consider and analyze the effect of having these implicit pairs in the data.

In Section 4.1, we analyze the performance of learning from implicit pairs in an unpaired setting by learning the mapping functions using  $\alpha$ -paired datasets with an unsupervised, unpaired algorithm which is completely unaware of the implicit pairs.

Technically, we learn the mapping functions  $G_{AB}$  and  $G_{BA}$  using  $\alpha$ -paired datasets in an unpaired setting, where the learning process is completely unaware to the implicit pairs. In Section 4.1, we analyze the performance of learning from implicit pairs, and show that a mix of unpaired and paired samples perform better in an unpaired setting.

### 3.3. Implicit pseudo-pairs

As discussed above, there are many situations where obtaining pairs is hard. However, in some cases, pseudo-pairs can be synthesized, see for example Figure 1. The question is whether these imperfect pairs, which only approximate real pairs, can be used as effective implicit pairs. To answer this question, we extend our  $\alpha$ -paired datasets to  $\alpha$ -pseudo-paired dataset where the pairing is carried out between *generated* pseudo-samples in domain A and real samples in domain B.

To augment the data, we assume we are provided with a model  $M(b) \approx a$  that takes samples  $b \in B$  and generates samples that approximate samples  $a \in A$ . The model  $M(b)$  can be interpreted as a simplification of the latent function  $G_{BA}$ . See Figure 1 for an illustration of pseudo-pairs in different datasets.

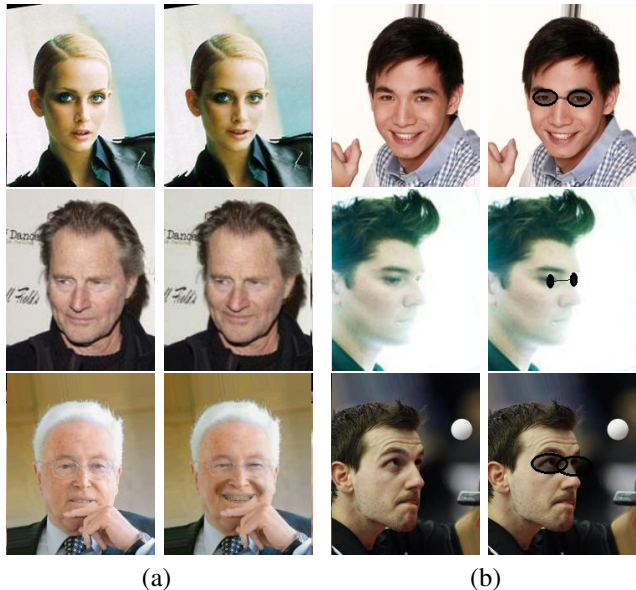


Figure 1: **illustration of pseudo-pairs.** (a) Pseudo-smiling and neutral faces (b) Pseudo-eyeglasses and faces without eyeglasses.

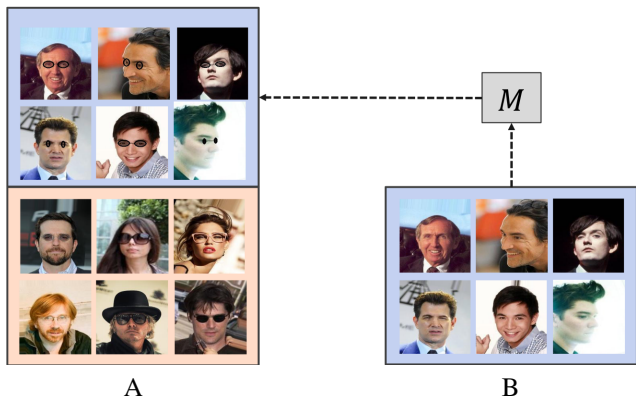


Figure 2: Learning using implicit pseudo-pairs with  $\alpha = 0.5$ . Given a model  $M(b)$ , we generate approximations of samples in domain B and augment them to domain A.

Figure 2 provides an overview of our approach in this setting. Given an unpaired dataset, we construct an  $\alpha$ -pseudo-paired dataset using a model  $M(b)$  to inject pseudo-samples to the unpaired sets. Note that in this asymmetric problem, where a model  $M(b)$  exists, the inverse mapping is of greater interest (as we can use  $M(b)$  to obtain analogous samples in domain A).

In the following section, we report on experiments that show that implicit pseudo-pairs boost the performance in the unpaired setting, and that using them as explicit pairs in a paired setting is significantly less effective.

$\alpha$	<i>Cityscapes</i>		<i>CVC-14</i>		<i>Facades</i>	
	A2B	B2A	A2B	B2A	A2B	B2A
0 (unpaired)	0.26	0.22	0.23	0.24	0.36	0.84
0.25	<b>0.24</b>	<b>0.21</b>	0.28	0.29	<b>0.33</b>	0.84
0.5	<b>0.24</b>	0.22	<b>0.22</b>	0.23	0.37	<b>0.80</b>
0.75	0.27	0.22	0.24	<b>0.22</b>	0.37	0.84
1 (paired)	0.25	0.22	0.23	0.25	<b>0.33</b>	0.87

Table 1: Reconstruction loss for different implicit pairing ratios,  $\alpha$ . lower is better. A2B is photo  $\rightarrow$  labels, B2A is labels  $\rightarrow$  photo.

$\alpha$	Per-pixel acc.	Per-class acc.	Class IOU
0	0.46	0.09	0.07
0.25	<b>0.69</b>	<b>0.20</b>	<b>0.15</b>
0.5	<b>0.69</b>	0.18	0.14
0.75	0.55	0.17	0.13
1	0.65	<b>0.20</b>	<b>0.15</b>

Table 2: FCN-scores for different implicit pairing ratios,  $\alpha$ , on Cityscapes labels $\rightarrow$ photo, higher is better. Remarkably using a mix of paired and unpaired samples is always better.

$\alpha$	Per-pixel acc.	Per-class acc.	Class IOU
0	0.571	0.132	0.100
0.25	0.657	0.138	0.108
0.5	<b>0.663</b>	<b>0.142</b>	<b>0.111</b>
0.75	0.582	0.141	0.108
1	0.658	0.141	0.110

Table 3: FCN-scores for different implicit pairing ratios,  $\alpha$ , on Cityscapes photo $\rightarrow$ labels, higher is better. Remarkably using a mix of paired and unpaired samples is always better.

## 4. Experiments and Results

### 4.1. The Power of Implicit Pairs

To validate our hypothesis that implicit pairs positively affect the result of training in the unpaired setting, we train a dual generator-discriminator architecture (CycleGAN) on  $\alpha$ -paired datasets composed of various image datasets. Specifically, we use the following paired datasets: Cityscapes [7], Facades [23] and CVC-14 [10], split the datasets into train and test sets and sample the train sets to generate various  $\alpha$ -paired dataset configurations. In all our experiments, we select  $|A| = |B|$  samples to generate balanced datasets.

To evaluate the performance on the test set, we measure the MSE between the generated images and their true coun-

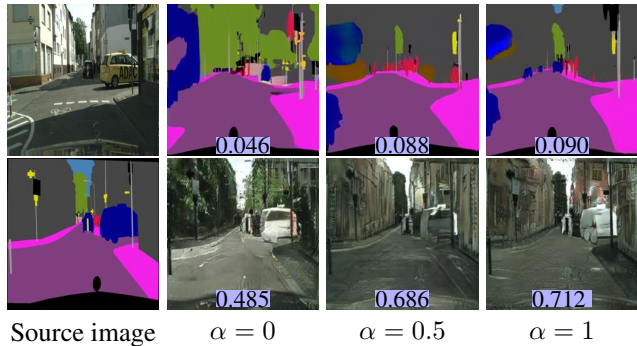


Figure 3: **Illustration of implicit pairs ratio experiments.** Pixel accuracy for a random test sample using models trained with varying pairing ratios.

terparts. Additionally we use the FCN-score metric introduced in [11] to evaluate the learned translations for the Cityscapes [7] dataset. Please refer to the supplementary material for more information regarding the evaluation metric and its use as well as additional information regarding the CycleGAN architecture and parameters used.

We report our evaluation in Tables 1, 2, 3. As can be expected, 1-paired datasets generally yield better performance than 0-paired datasets with an average improvement of 14.2%. Even more interesting is the fact that having even a few paired samples improves the results dramatically compared to having no pairs at all. Remarkably it seems that in most cases using a completely paired dataset is not the best option. Instead using a mix of paired and unpaired samples is usually a better strategy, surpassing completely paired datasets on average by 3.4%. In Figure 3, we illustrate a random sample from the Cityscapes dataset and its results given different training dataset configurations. Refer to supplementary material for more results.

### 4.2. Pseudo-Pairs for Implicit Learning

In the previous section, we demonstrated that implicit pairs positively affect the results of image-to-image translation problems. However, in most cases, it is difficult, or unreasonable, to obtain such paired samples. Therefore, we explore a more challenging, yet applicable, setting where the pairs do not originate from real samples. In this setting, we assume we are provided with a model  $M(b)$ , as described in Section 3.2, that generates samples which approximate samples in the analogous domain  $A$ .

Our approach is to generate, for each sample in domain  $B$ , a paired pseudo-sample using  $M(b)$  and use it to augment the samples in domain  $A$ . This creates pseudo-paired datasets with a 50% pairing ratio. An overview of this method is shown in Figure 2.

For the experiments on pseudo-pairs, we use the CelebA

dataset [18]. We generate two different types of pseudo  $\alpha$ -paired datasets on which we evaluate our method: (i) faces with and without eyeglasses and (ii) smiling and neutral faces. The datasets can be obtained using the labeling information available for each image in the CelebA dataset. In (i), we generate pseudo-samples with eyeglasses using simple heuristics. Using the available facial landmarks, we generate ellipses around the eyes by sampling a random height  $h$  in the range of  $[10, 25]$  pixels, a random width in the range of  $[h/2, 2 \cdot h]$  and a transparency coefficient in the range  $[0.1, 1.0]$ . The two ellipses are connected by a line with the same transparency and with width in the range of  $[h/5, h/2]$ . In (ii), we use the technique of Averbuch et al. [4] to generate smiling pseudo-samples. It is important to note that in both cases, it is significantly more challenging to generate clean samples in the inverse direction. See Figure 1 for an illustration of pseudo-pairs in both types of datasets.

Assessing the quality of trained GAN models is difficult. One of the reasons for this is that they can accomplish their prescribed goals in ways that defy the expected behavior. For example, when learning to remove eyeglasses, the model could learn to replace the face with another face that is not wearing eyeglasses instead of removing them while retaining the identity of the original person. To measure robustness against learning non-meaningful mappings, we would like to measure how successful the mapping is in retaining the expressiveness of the original sample which is not correlated to the task at hand.

Following previous works that use the MSE in representation space as either a perceptual or an identity loss term [27, 2, 15, 13, 25], we use a representation-space similarity measure,  $\text{InfoSim}$ , to measure the preservation of information not related to the task between the input sample and its generated counterpart. In the case of facial translation tasks, we would like to measure how well the facial identity is preserved after the translation. For that end, we use the representations learned by the OpenFace network [1]. This network is trained for facial recognition and as we show in Figure 9 is invariant to transient features, such as smiling or wearing eyeglasses. To measure the similarity we use the MSE between the representation of the input and output images.

**Pseudo-pairs experimental setup.** In our experiments, we sample 1000 unpaired samples from CelebA [18] from each domain, which we augment with another 1000 samples according to the augmentation method used in the specific experiment. The resolution of the images is 128X128. Unless stated otherwise, all of the experiments were done using the CycleGAN model described above.

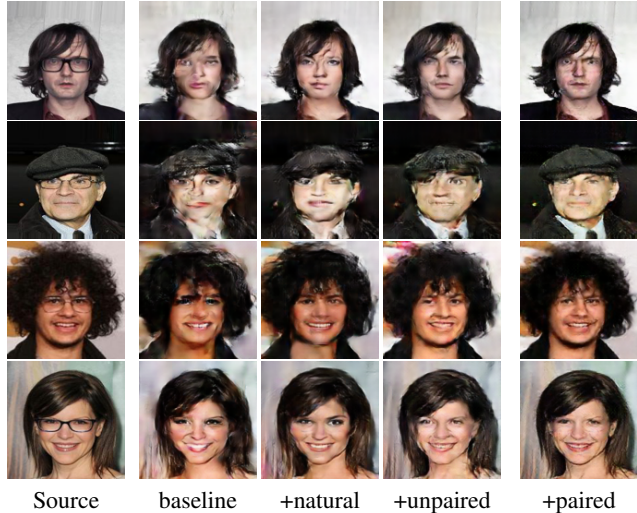


Figure 4: *Eyeglass removal* results using different dataset configurations. Above we illustrate our results (on the right) compared against three augmentation baselines, described in Section 4.2

**Comparing implicit pseudo-pairs to baseline methods.**

We evaluate our pseudo-pairs augmentation technique against three augmentation baselines: (i) no-augmentation, (ii) pseudo-unpaired augmentation and (iii) *natural* augmentation of real images belonging to the corresponding domain. In (i), we do not augment the basic dataset configuration with any samples. In (ii), we augment the basic dataset configuration with pseudo-samples whose paired real samples are not in the dataset. In (iii), we simply augment the basic dataset configuration with more real images, sampled from the full dataset.

The  $\text{InfoSim}$  results for the baseline methods are reported in Table 4. Figures 4, 5 demonstrate the results of these experiments. As the results illustrate, using implicit pseudo-pairs improves the quality of the translation while better preserving the facial identity. For instance, it is especially noticeable that using implicit pseudo-pairs introduces fewer artifacts in comparison to the other approaches.

Task	ours	(i)	(ii)	(iii)
Smile	<b>0.00160</b>	0.00365	0.00282	0.00372
Eyeglass	<b>0.00181</b>	0.00482	0.00313	0.00418

Table 4:  $\text{InfoSim}$  comparison with the baseline augmentation methods described in Subsection 4.2. Lower is better.

**Pseudo-pairs ratio analysis.** In Section 4.1, we demonstrated that having different ratios of pairs in the dataset can have a significant effect on the results. Here we continue this line of inquiry by evaluating the effect differ-

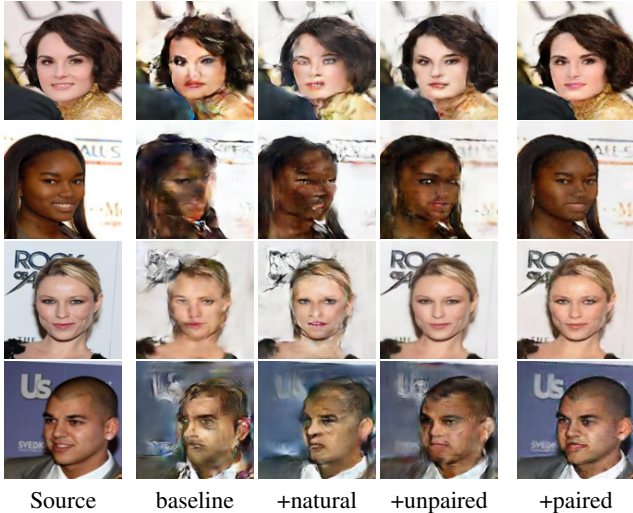


Figure 5: Results for the *smile removal* task using different dataset configurations. Above we illustrate our results (on the right) compared against three augmentation baselines, described in Section 4.2.

ent ratios of pseudo-pairs have. We test the following  $\alpha$ -paired configurations:  $\alpha = 0.25, 0.5, 0.75, 1.0$ . To create a  $\alpha = 0.25$  pseudo-paired dataset, half of the augmentation samples are paired and the other half are unpaired. To create datasets with a pairing ratio higher than 50% we remove domain A samples from the initial dataset and augment with more pseudo-pairs. For example, the **0.75**-pseudo-paired dataset has 500 unpaired real samples augmented with 1500 pseudo-pairs. The InfoSim results for these experiments are reported in Table 5. The results clearly demonstrate that the more pairs we have in the dataset, the better the identity is preserved. The qualitative results for these experiments are demonstrated in Figures 6, 7. As the figure illustrates, although having more pairs allows us to better preserve the facial identity, it also reduces the ability of the model to learn the task itself. We propose that this occurs because as the model is exposed to more pseudo-pairs it is also exposed to fewer examples of the real domain and thus is less able to generalize to the real task. This is especially pronounced in the *smile removal* task as the generation model  $M(b)$  is based on a closed set of smile templates and generalizing from that limited set is hard.

**Task completion user study.** To further quantify the success of different ratios, we conduct a user study in which participants are presented with translated results generated using models trained with 0%, 50% and 100% pseudo-paired datasets and asked which model completes the task better. To allow for fine-grained comparison, the participants are shown the results of only two models at a time

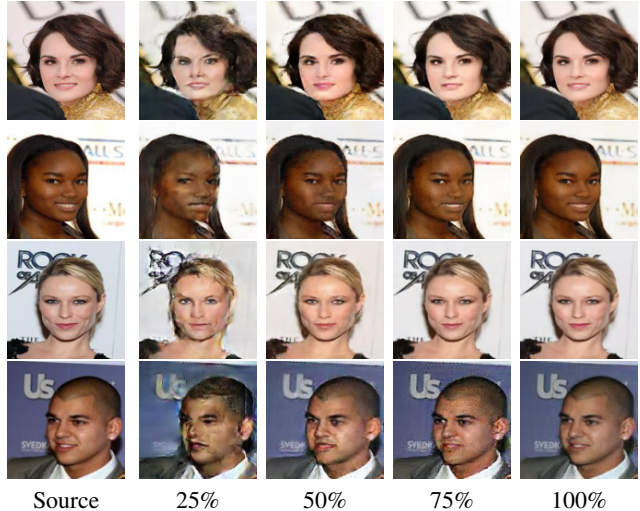


Figure 6: Pseudo-pair ratio analysis for the *smile removal* task. Above we illustrate a few results using various pairing ratios. As the figure illustrates, using a 50% pairing configuration yields identity-preserving results which still perform the task (smile removal in this case) better than a higher pairing ratio.

(or one model and the source image) to choose one, both or none if both are equally good or bad.

We had a total of 43 participants which completed separate studies for 50 eyeglass wearing and 41 smiling samples.

In Table 6 we report the rate by which participants preferred one model over the other. It is clear that using a 50% pseudo-paired yields the best results in terms of task completion.

Task	0.25-Paired	0.5-Paired	0.75-Paired	1-Paired
Smile	0.00293	0.00160	0.00093	<b>0.00025</b>
Eyeglass	0.00153	0.00181	0.00110	<b>0.00025</b>

Table 5: InfoSim values for pairing ratios experiments. Lower is better.

	Rejected	0%	50%	100%
Preferred				
0% (Smile)	-	0.257	0.486	
50% (Smile)	<b>0.742</b>	-	<b>0.663</b>	
100% (Smile)	0.513	0.336	-	
0% (Eyeglass)	-	0.264	0.915	
50% (Eyeglass)	<b>0.735</b>	-	<b>1.0</b>	
100% (Eyeglass)	0.084	0.0	-	

Table 6: Task completion preference rate according to the user study

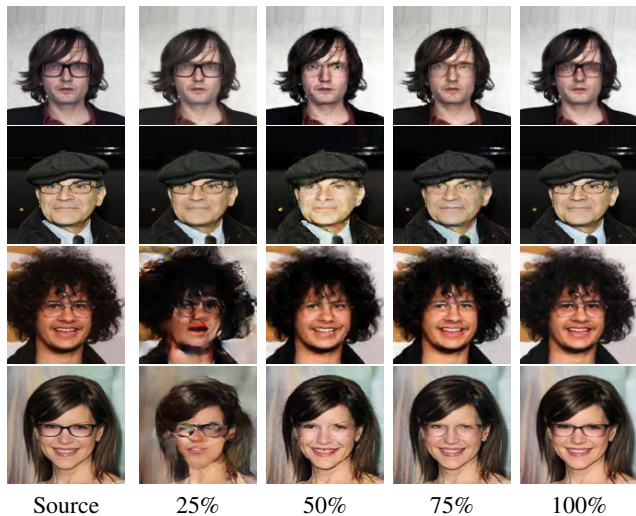


Figure 7: Pseudo-pair ratio analysis for the *eyeglass removal* task. Above we illustrate a few randomly selected results using various pairing ratios. As the figure illustrates, using a 50% pairing configuration yields reasonable identity-preserving results while perform the task (eyeglass removal in this case) better than a higher pairing ratio.

**Pseudo-pairs in different image-to-image translation settings.** In previous experiments we have used the generated pseudo-pairs in an implicit fashion. To understand more fully the effect the pairs have on training of models we further experiment with using them in an explicit setting. For explicit training we use the previously mentioned Pix2Pix model [11] with the completely pseudo-paired dataset and compare it against the our 0.5-pseudo-paired implicitly trained results. From the  $\text{InfoSim}$  numbers in Table 7 and the qualitative results in Figure 8 it is clear that the explicit approach barely changes the input, thus achieving a very low  $\text{InfoSim}$  values while not actually completing the task.

We suggest that this because in the explicit experiment is completely pseudo-paired, i.e. there are no real samples of eyeglass images which leads the model to overfit to the dataset and particularly to the features of the pseudo-glasses which are different from real eyeglasses. This prevents it from generalizing to the real eyeglasses in the test set.

This suggests that as long as the generation model  $M(b)$  is not perfect, it would introduce features that the explicit method will overfit on, and the only efficient way to use the pseudo-samples might be in an implicit manner. In our Discussion section we explore the effect the artifacts introduced by  $M(b)$  to the dataset has on the learned mappings.

Implicit	Explicit
0.00180	<b>0.000342</b>

Table 7:  $\text{InfoSim}$  values for explicit and implicit experiments on the *Eyeglass removal* task. Lower is better.



Figure 8: *Eyeglass removal* with pseudo-pairs in different settings. Above we illustrate a few randomly selected results by models trained using either an explicit ([11]) and implicit ([29]) settings. As the figure illustrates, an implicit setting leads to the best and most consistent results.

## 5. Discussion and Conclusions

In Section 4.2 we demonstrate that augmenting the dataset with implicit pseudo-pairs boosts the performance of image-to-image translation models. In what follows, we further discuss and analyze the importance of the implicit pseudo-pairs in the unpaired image-to-image translation setting. We argue that these pseudo-pairs introduce an implicit mapping from which the model is able to learn a better inverse mapping.

It is important to note that while our results suggests that a 50% pairing ratio strikes a good balance between identity conservation and task completion, in this paper we do not

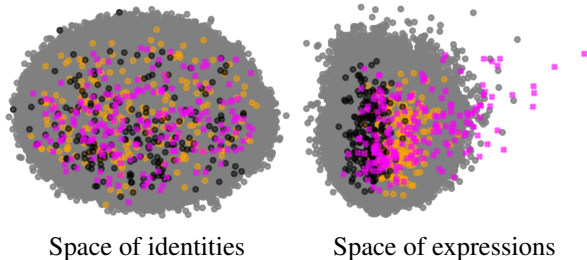


Figure 9: Pseudo-pairs visualized on representations not related to the task (space of identities) and representations related to the task (space of expressions) for the *smile removal* task. Above we use PCA to visualize smiling (in orange), neutral (in black) and augmented (in fuchsia), training samples.

advocate for a specific  $\alpha$  pairing ratio. Instead we show that for every dataset and task there is a trade off between identity preservation (i.e., a low InfoSim score) and the task completion which needs to be explored. In Section 4.1, we show that having a mixture of paired and unpaired samples consistently gives the best result and based on the results in Section 4.2 we propose that these is true for pseudo-pairs as well.

To better understand the effect of the pseudo-pairs, we visualize the training and generated samples using several representations. We represent *the space of identities* using the OpenFace representation described in the previous section. *The space of expressions* is represented using a simple classifier trained on a subset of CelebA to distinguish between smiling and neutral images. We fit a PCA model on representations extracted for the entire celebA dataset [18] and project these representations onto a 2D space.

**Pseudo-pairs as training samples.** In Figure 9 we visualize both representations on the training data. As the figure illustrates, the distribution of the pseudo-samples is very similar to those of the smiling and neutral face distributions in respect to the space of identities, demonstrating that in terms of attributes not related to the translation task the pseudo-samples are indistinguishable from the real samples. The distribution of the expression representation, on the other hand, shows that the generation model  $M(b)$  creates images that do not conform to the general CelebA distribution (as they are clearly mapped outside the space spanned by the smiling samples). While this is not surprising, as the pseudo-samples are, by definition, imperfect, it does raise the question of how these imperfect pseudo-samples positively affect the learned mapping.

**Samples generated using various augmentation settings.** To address the aforementioned question, we visualize the

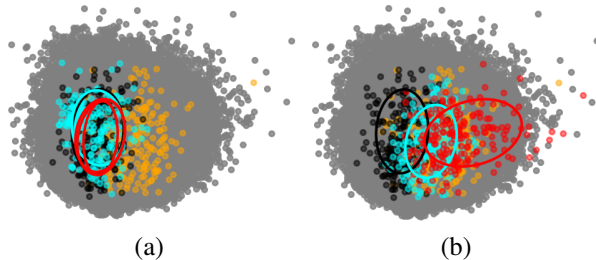


Figure 10: *Smile removal* test result distributions. (a) Comparison of pseudo-paired augmentation in cyan and fitted ellipses for the baseline methods in red. (b) Distribution of test results when training Pix2Pix (in red) and CycleGAN (in cyan) with a 100% pseudo-paired dataset

samples generated from the images belonging to the test set. We show the distribution created using the implicit pseudo-pairs method in Figure 10. To emphasize the correlation between the translated samples and the real samples in the target “neutral” domain, we fit ellipses to both sets. We compare these with ellipses fitted to the translation results of the baseline methods introduced in Section 4.2. As the figure illustrates, the learned translation for all baseline settings is somewhat similar, but the translation learned in the paired setting is significantly more distinct and creates samples which are classified more strongly as “neutral”. To better quantify the differences, we measure the Euclidean distance between the center of the ellipse of the real samples and the center of the generated ones, as well as the average difference ratio between the major and minor axes. Our method obtains a Euclidean distance of 0.269 between the centers and an average difference ratio of 6% between the axes, while for the closest baseline the Euclidean distance to the real center is 1.172 and the average difference ratio with the real axes is 11%. This result illustrates that the model is able to detect the latent implicit signal within the dataset.

On the right of Figure 10, we compare the learned distributions of a completely pseudo-paired dataset learned either explicitly (with Pix2Pix) or implicitly (with CycleGAN). As discussed earlier, both implicit and explicit learning settings fail at completing the task (smile removal in this case) when trained over a completely pseudo-paired dataset. This is also evident in the figure, as the generated samples are not mapped to where real “neutral” images are mapped. As the figure illustrates, the implicit architecture seems to overfit to the identity signal which is implicitly provided in the pairs. On the other hand, the explicit architecture yields samples which are not spanned by the real images in the test set, and resembles the behavior of the pseudo-samples, as illustrated in Figure 9. This demonstrates that the explicit model is more strongly influenced by the noisy signal introduced by the pseudo-pairs.

**Conclusions.** It is well established that many of the most fundamental human abilities are learned implicitly. In this work, we analyzed the positive effect of learning with implicitly paired samples in an image-to-image translation problem. We have shown, through numerous experiments and examples, that learning from implicit pairs can effectively guide the network to learn a better mapping, more than additional unpaired or random samples.

We further analyzed the power of implicit learning using pseudo-pairs. These pseudo-pairs can be obtained automatically either using simple geometric models, as we have shown in the case of faces augmented with eyeglasses, or by more complicated models, such as neutral faces augmented with smiles. In both cases, implicitly providing the network with these pairs yields plausible mappings that better preserve non-task related information. Additionally, we have shown that datasets augmented with pseudo-pairs can be significantly more effective in an implicit setting than in an explicit one.

The fact that the contribution of the implicit pairs is effective despite their signal being hidden across the dataset, raises the question of what other types of implicit signals may a deep neural network exploit effectively. In the future, we believe that exploring the mechanisms by which neural networks learn from implicit signals may shed light on the understanding of how neural networks learn in general and allow for finer control in the configuration of datasets.

## References

- [1] Brandon Amos, Bartosz Ludwiczuk, and Mahadev Satyanarayanan. Openface: A general-purpose face recognition library with mobile applications. Technical report, CMU-CS-16-118, CMU School of Computer Science, 2016.
- [2] Grigory Antipov, Moez Baccouche, and Jean-Luc Dugelay. Face aging with conditional generative adversarial networks. *CoRR*, abs/1702.01983, 2017.
- [3] Antreas Antoniou, Amos Storkey, and Harrison Edwards. Data Augmentation Generative Adversarial Networks. *arXiv e-prints*, page arXiv:1711.04340, Nov. 2017.
- [4] Hadar Averbuch-Elor, Daniel Cohen-Or, Johannes Kopf, and Michael F Cohen. Bringing portraits to life. *ACM Transactions on Graphics (TOG)*, 36(6):196, 2017.
- [5] Richárd Bellon, Younggeon Choi, Nikoletta Ekker, Vincent Lepetit, L. Mike Olasz, Daniel Sonntag, Zoltán Tószér, Kyounghwan Yoo, and András Lőrincz. Model based augmentation and testing of an annotated hand pose dataset. In Gerhard Friedrich, Malte Helmert, and Franz Wotawa, editors, *KI 2016: Advances in Artificial Intelligence*, pages 17–29, Cham, 2016. Springer International Publishing.
- [6] Sagie Benaïm and Lior Wolf. One-sided unsupervised domain mapping. *CoRR*, abs/1706.00826, 2017.
- [7] Marius Cordts, Mohamed Omran, Sebastian Ramos, Timo Rehfeld, Markus Enzweiler, Rodrigo Benenson, Uwe Franke, Stefan Roth, and Bernt Schiele. The cityscapes dataset for semantic urban scene understanding. In *Proc. of the IEEE Conference on Computer Vision and Pattern Recognition (CVPR)*, 2016.
- [8] Maayan Frid-Adar, Idit Diamant, Eyal Klang, Michal Amitai, Jacob Goldberger, and Hayit Greenspan. Gan-based synthetic medical image augmentation for increased CNN performance in liver lesion classification. *CoRR*, abs/1803.01229, 2018.
- [9] Zhe Gan, Liqun Chen, Weiyao Wang, Yunchen Pu, Yizhe Zhang, Hao Liu, Chunyuan Li, and Lawrence Carin. Triangle generative adversarial networks. *CoRR*, abs/1709.06548, 2017.
- [10] Alejandro González, Zhijie Fang, Yainuvis Socarras, Joan Serrat, David Vázquez, Jiaolong Xu, and Antonio M. López. Pedestrian detection at day/night time with visible and infrared cameras: A comparison. *Sensors*, 16(6), 2016.
- [11] Phillip Isola, Jun-Yan Zhu, Tinghui Zhou, and Alexei A. Efros. Image-to-image translation with conditional adversarial networks. *CoRR*, abs/1611.07004, 2016.
- [12] Cheng-Bin Jin, Wonmo Jung, Seongsu Joo, Ensik Park, Ahn Young Saem, In Ho Han, Jae-Il Lee, and Xuenan Cui. Deep CT to MR synthesis using paired and unpaired data. *CoRR*, abs/1805.10790, 2018.
- [13] Justin Johnson, Alexandre Alahi, and Fei-Fei Li. Perceptual losses for real-time style transfer and super-resolution. *CoRR*, abs/1603.08155, 2016.
- [14] Taeksoo Kim, Moonsoo Cha, Hyunsoo Kim, Jung Kwon Lee, and Jiwon Kim. Learning to discover cross-domain relations with generative adversarial networks. *CoRR*, abs/1703.05192, 2017.
- [15] Christian Ledig, Lucas Theis, Ferenc Huszar, Jose Caballero, Andrew P. Aitken, Alykhan Tejani, Johannes Totz, Zehan Wang, and Wenzhe Shi. Photo-realistic single image super-resolution using a generative adversarial network. *CoRR*, abs/1609.04802, 2016.
- [16] Chongxuan Li, Kun Xu, Jun Zhu, and Bo Zhang. Triple generative adversarial nets. *CoRR*, abs/1703.02291, 2017.
- [17] Ming-Yu Liu, Thomas Breuel, and Jan Kautz. Unsupervised image-to-image translation networks. *CoRR*, abs/1703.00848, 2017.
- [18] Ziwei Liu, Ping Luo, Xiaogang Wang, and Xiaoou Tang. Deep learning face attributes in the wild. In *Proceedings of International Conference on Computer Vision (ICCV)*, 2015.
- [19] Giovanni Mariani, Florian Scheidegger, Roxana Istrate, Costas Bekas, and Cristiano Malossi. BAGAN: Data Augmentation with Balancing GAN. *arXiv e-prints*, page arXiv:1803.09655, Mar. 2018.
- [20] Leon Sixt, Benjamin Wild, and Tim Landgraf. RenderGAN: Generating Realistic Labeled Data. *arXiv e-prints*, page arXiv:1611.01331, Nov. 2016.
- [21] Soumya Tripathy, Juho Kannala, and Esa Rahtu. Learning image-to-image translation using paired and unpaired training samples. *CoRR*, abs/1805.03189, 2018.
- [22] Nicholas J. Tustison, Brian B. Avants, Zixuan Lin, Xue Feng, Nicholas Cullen, Jaime F. Mata, Lucia Flors, James C. Gee, Talissa A. Altes, III John P. Mugler, and Kun Qing. Convolutional neural networks with template-based data augmentation for functional lung image quantification. *Academic Radiology*, 2018.

- [23] Radim Tyleček and Radim Šára. Spatial pattern templates for recognition of objects with regular structure. In Proc. GCPR, Saarbrücken, Germany, 2013.
- [24] Hristina Uzunova, Matthias Wilms, Heinz Handels, and Jan Ehrhardt. Training cnns for image registration from few samples with model-based data augmentation. In Maxime Descoteaux, Lena Maier-Hein, Alfred Franz, Pierre Jannin, D. Louis Collins, and Simon Duchesne, editors, Medical Image Computing and Computer Assisted Intervention MICCAI 2017, pages 223–231, Cham, 2017. Springer International Publishing.
- [25] Chaoyue Wang, Chang Xu, Chaohui Wang, and Dacheng Tao. Perceptual adversarial networks for image-to-image transformation. CoRR, abs/1706.09138, 2017.
- [26] Yu-Xiong Wang, Ross B. Girshick, Martial Hebert, and Bharath Hariharan. Low-shot learning from imaginary data. CoRR, abs/1801.05401, 2018.
- [27] Hongyu Yang, Di Huang, Yunhong Wang, and Anil K. Jain. Learning face age progression: A pyramid architecture of gans. CoRR, abs/1711.10352, 2017.
- [28] Zili Yi, Hao Zhang, Ping Tan, and Minglun Gong. Dualgan: Unsupervised dual learning for image-to-image translation. CoRR, abs/1704.02510, 2017.
- [29] Jun-Yan Zhu, Taesung Park, Phillip Isola, and Alexei A. Efros. Unpaired image-to-image translation using cycle-consistent adversarial networks. CoRR, abs/1703.10593, 2017.

## Architectures

### CycleGAN

In all of our experiments with CycleGAN we have used the vanilla architecture that they have used with 9 residual blocks. Following the naming conventions used in [29] we express the generator layer parameters as follows: Define a  $7 \times 7$  Convolution-InstanceNorm-ReLU layer with  $k$  filters and stride 1 as  $c7s1-k$ , a  $3 \times 3$  Convolution-InstnceNorm-ReLU layer with  $k$  filters and stride 2 as  $dk$ , a residual block with  $3 \times 3$  convolutional layers with equal numbers of filters on both layers as  $Rk$  and a  $3 \times 3$  fractional-stridded-Convolution-InstanceNorm-ReLU layer with  $k$  filers and stride  $1/2$  as  $uk$ . For the discriminator we denote a  $4 \times 4$  Convolution-InsanceNorm-LeakyReLU layer with  $k$  filters and stride 2 with  $Ck$ .

Using these definitions the generator network can be expressed as:

$c7s1 - 64, d128, d256, R256, R256, R256,$   
 $R256, R256, R256, R256, R256, R256,$   
 $u128, u64, c7s1 - 3$

The discriminator network can be similarly expressed as:

$C64 - C128 - C256 - C512.$

### Pix2Pix

All experiments involving the Pix2Pix architecture were done using the vanilla version as well. Using the conventions used in [11] for the Pix2Pix network we denote the Convolution-BatchNorm-ReLU layer with  $k$  filters as  $Ck$  and the Convolution-BatchNorm-Dropout-ReLU layer with 50% dropout rate as  $k$  filters as  $CDk$ .

The generator is comprised of an encoder expresses as:  
 $C64 - C128 - C256 - C512 - C512 - C512 - C512 - C512$   
and a decoder expressed as:

$CD512 - CD512 - CD512 - C512 - C256 - C128 - C64$

The discriminator can be expressed as:

$C64 - C128 - C256 - C512$

### FCN-score

**photo**  $\rightarrow$  **labels** To convert the generated image to a label matrix we mapped every pixel's rgb value to the label with the lowest mean distance according to the label  $\leftrightarrow$  rgb value conversion table provided with the Cityscapes [7] dataset.

**labels**  $\rightarrow$  **photo** In this direction we use the same FCN-8 network that was used in [11] to segment the generated image into a label matrix.

Finally in either direction we used the evaluation script provided in Zhu's github repository <sup>1</sup>

### CVC-14 dataset

The dataset contains paired sequences of road scenes taken during the day and during the night. To break the temporal dependence between the frames we only sample every 100-th frame from the day sequences.

---

<sup>1</sup><https://github.com/junyanz/pytorch-CycleGAN-and-pix2pix>



Source

$\alpha = 0$

$\alpha = 0.25$

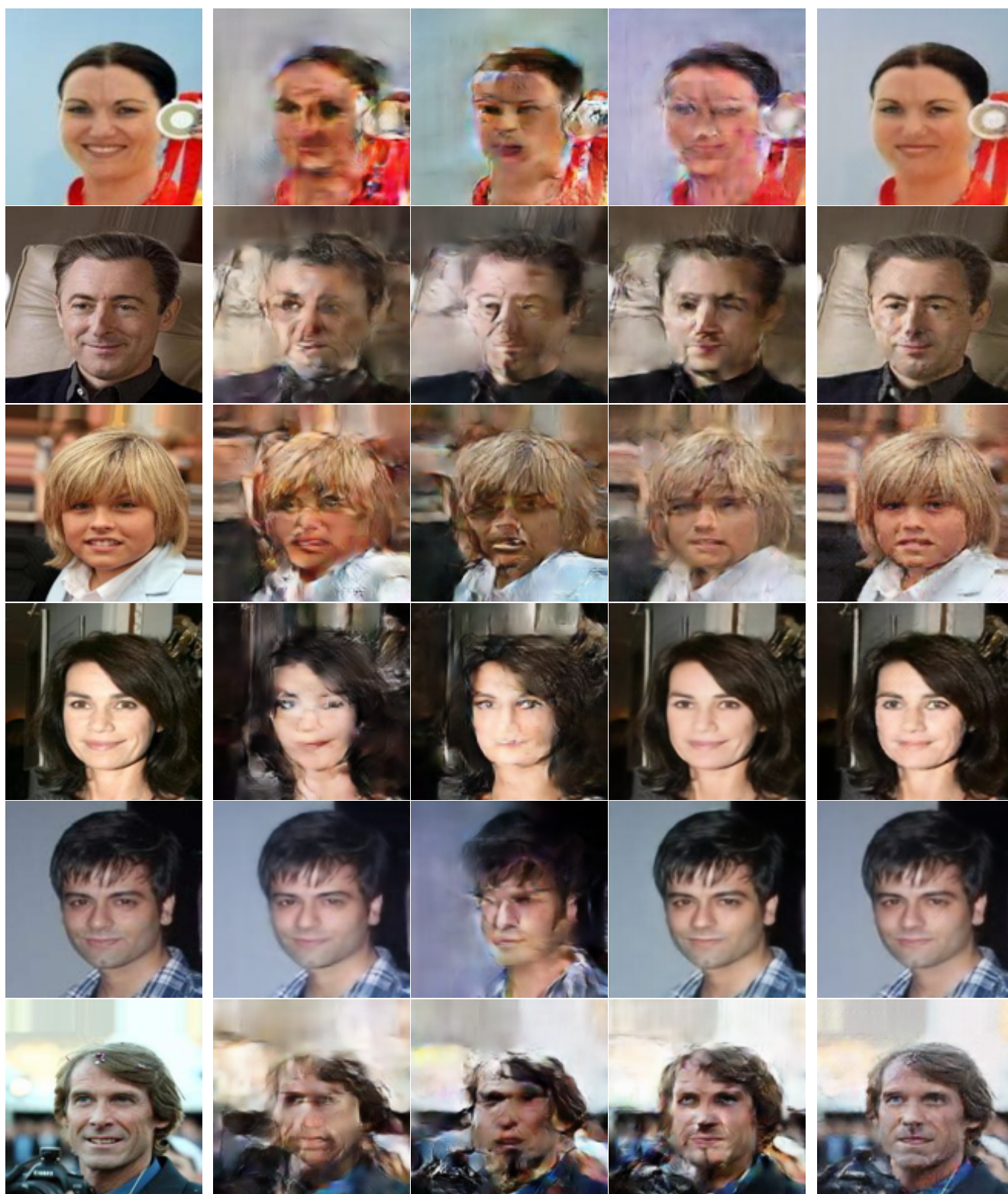
$\alpha = 0.5$

$\alpha = 0.75$

$\alpha = 1$



Figure 11: Additional examples of the effect of learning image-to-image translation with varying pairing ratios



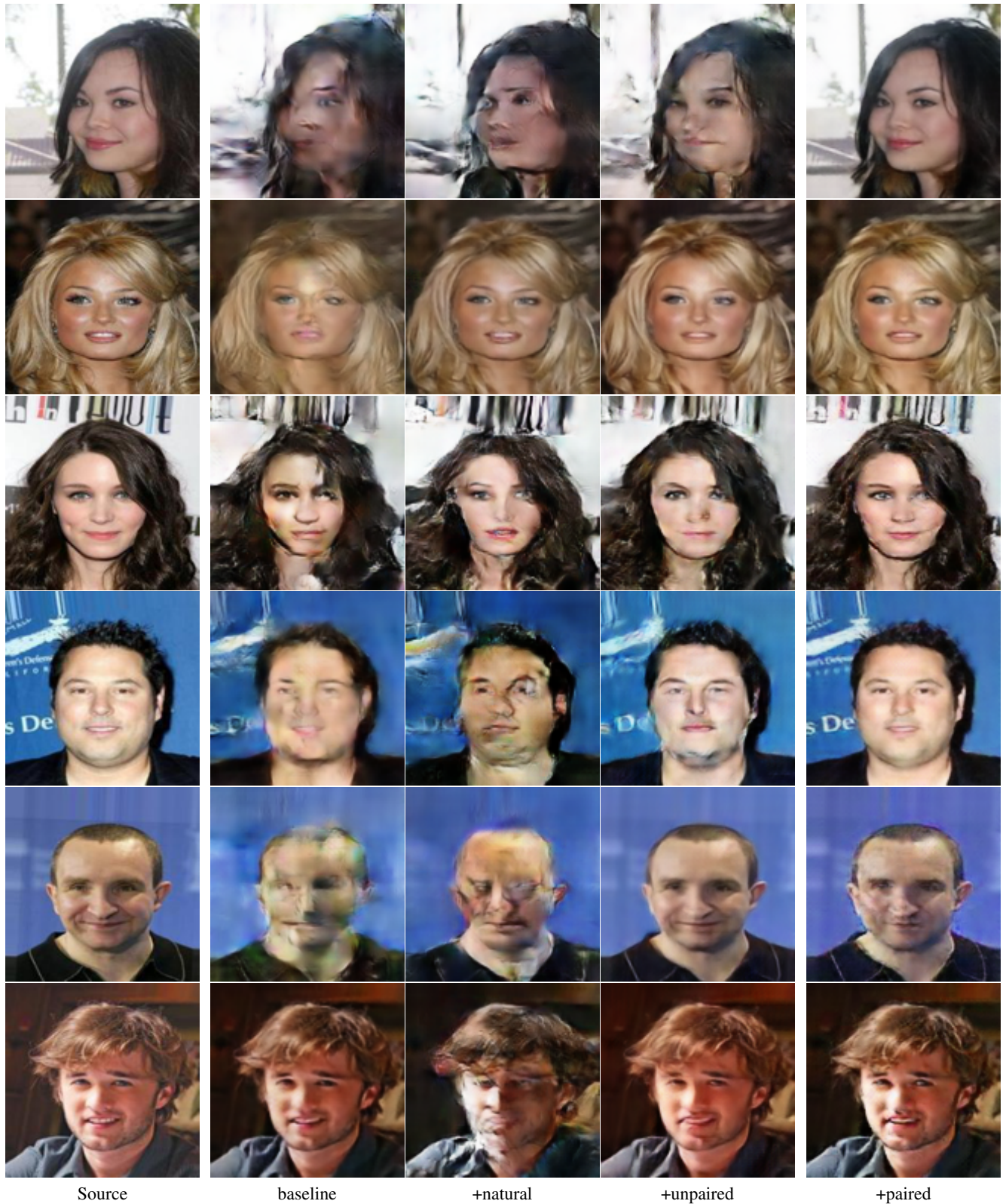
Source

baseline

+natural

+unpaired

+paired



Source

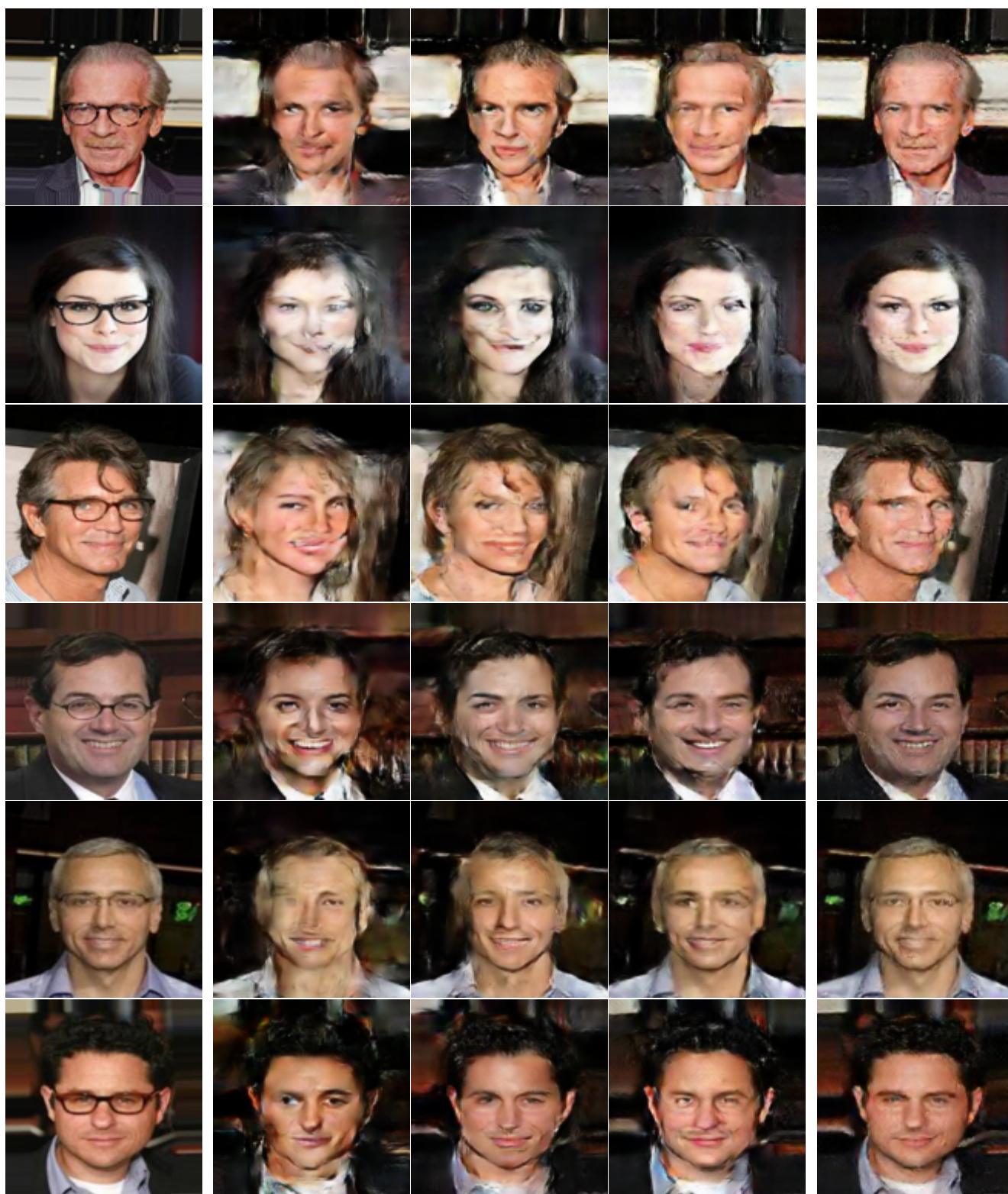
baseline

+natural

+unpaired

+paired

Figure 12: Additional results for the smile removal task using different dataset configurations. Above we illustrate our randomly selected results (on the right) compared against three augmentation baselines, described in Section 4.2.



Source

baseline

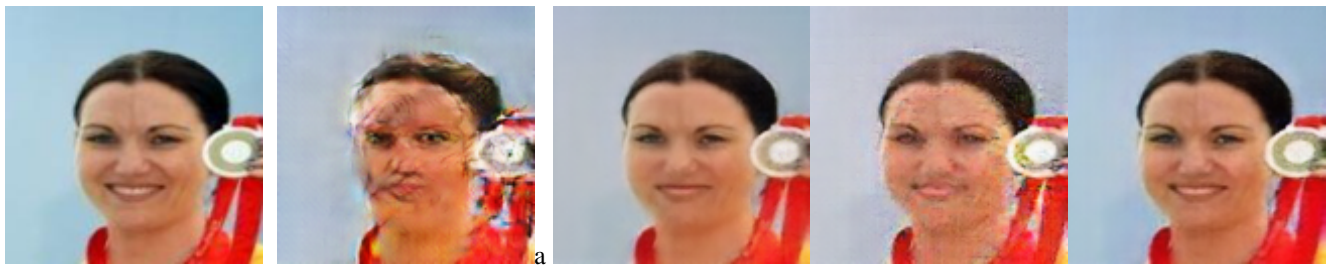
+natural

+unpaired

+paired



Figure 13: Additional Eyeglass removal results using different dataset configurations. Above we illustrate our randomly selected results (on the right) compared against three augmentation baselines, described in Section 4.2



1



Source

25%

50%

75%

100%

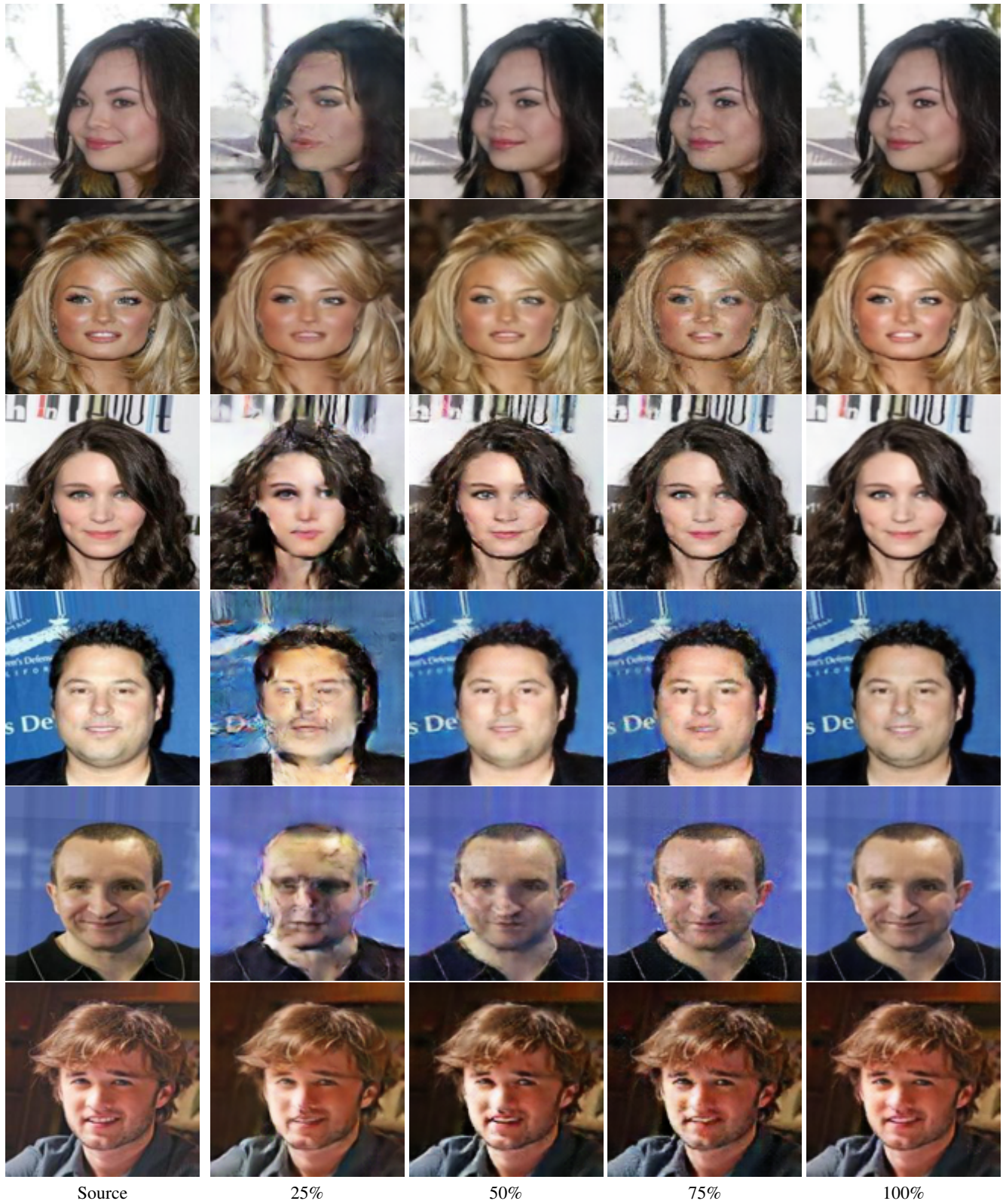


Figure 14: Additional pseudo-pair ratio analysis results for the smile removal task



Source

25%

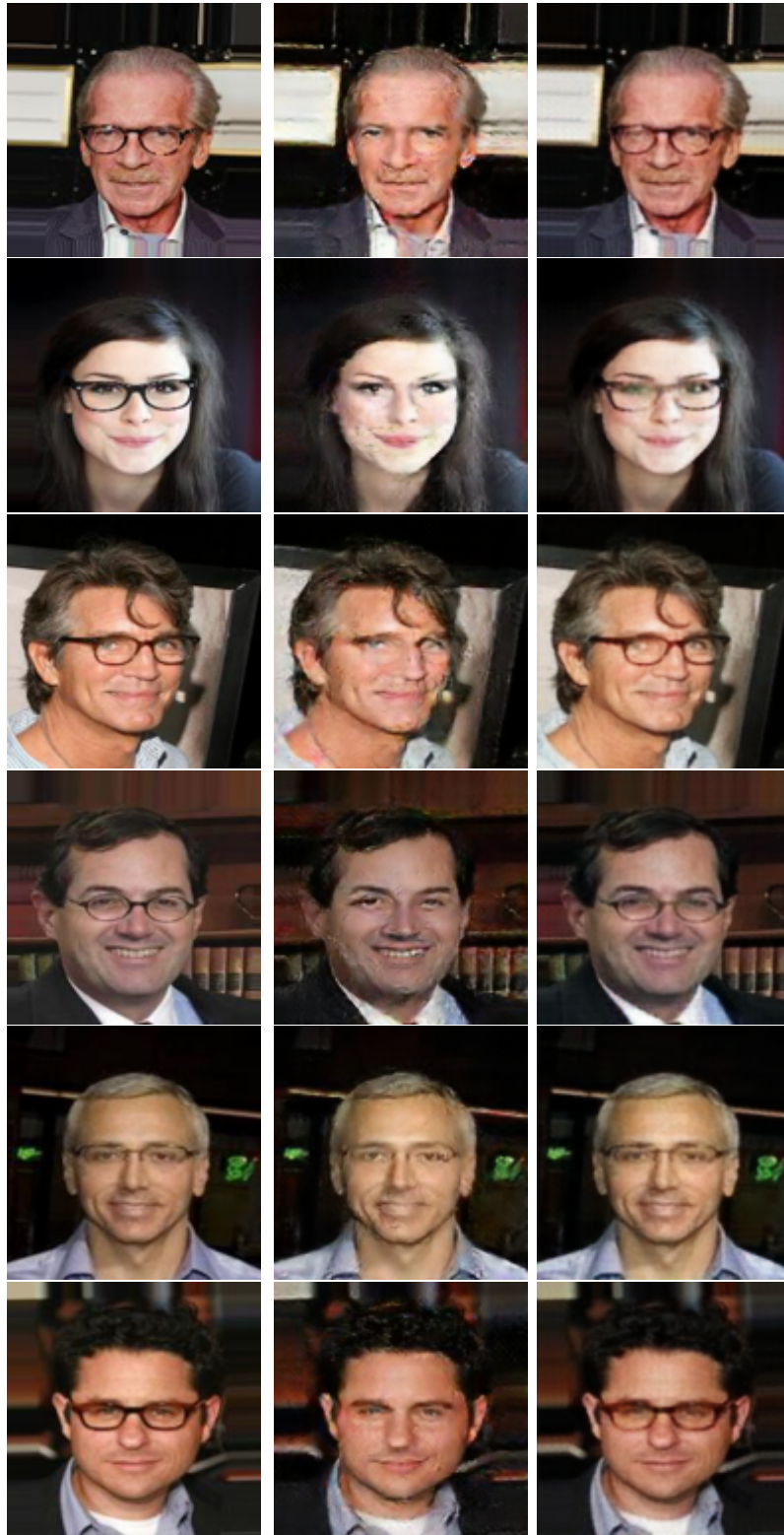
50%

75%

100%



Figure 15: Additional pseudo-pair ratio analysis results for the eyeglass removal task



Source

Implicit

Explicit



Figure 17: Additional Eyeglass removal results with pseudo-pairs in different settings.